JACS
JOURNAL OF THE AMERICAN CHEMICAL SOCIETY

Article

pubs.acs.org/JACS

Design of Asymmetric Particles Containing a Charged Interior and a Neutral Surface Charge: Comparative Study on *in Vivo* Circulation of Polyelectrolyte Microgels

Kai Chen,[†] Jing Xu,[‡] J. Christopher Luft,[‡,§,∥] Shaomin Tian,[‡,§] Jay S. Raval,[⊥] and Joseph M. DeSimone*[,†,‡,§,∥,#,⊗,∇]

[†]Department of Chemistry, [‡]Lineberger Comprehensive Cancer Center, [§]Institute for Nanomedicine, [∥]School of Pharmacy, [⊥]Department of Pathology and Laboratory Medicine, [#]Institute for Advanced Materials, University of North Carolina, Chapel Hill, North Carolina 27599, United States

[⊗]Department of Chemical and Biomolecular Engineering, North Carolina State University, Raleigh, North Carolina 27695, United States

[∇]Sloan-Kettering Institute for Cancer Research, Memorial Sloan-Kettering Cancer Center, New York, New York 10065, United States

Supporting Information

ABSTRACT: Lowering the modulus of hydrogel particles could enable them to bypass *in vivo* physical barriers that would otherwise filter particles with similar size but higher modulus. Incorporation of electrolyte moieties into the polymer network of hydrogel particles to increase the swelling ratio is a straightforward and quite efficient way to decrease the modulus. In addition, charged groups in hydrogel particles can also help secure cargoes. However, the distribution of charged groups on the surface of a particle can accelerate the clearance of particles. Herein, we developed a method to synthesize highly swollen microgels of precise size with near-neutral surface charge while retaining interior charged groups. A strategy was employed to enable a particle to be highly cross-linked with very small mesh size, and subsequently PEGylated to quench the exterior amines only without affecting the internal amines. Acidic degradation of the cross-linker allows for swelling of the particles to microgels with a desired size and deformability. The microgels fabricated demonstrated extended circulation *in vivo* compared to their counterparts with a charged surface, and could potentially be utilized in *in vivo* applications including as oxygen carriers or nucleic acid scavengers.

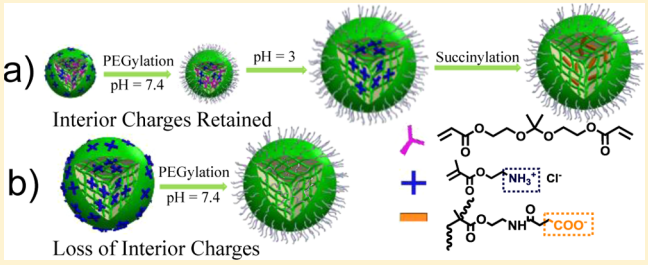

INTRODUCTION

Hydrogels are promising biomaterials extensively explored in both tissue engineering and drug delivery because of their hydrophilicity and biocompatibility.[1] When the size of hydrogels is downscaled to the micro- and nanoregime, the resulting particles can potentially be engineered for intravascular delivery of therapeutics.[2,3] Polyelectrolytes containing groups such as carboxylic acid or amines are often incorporated into micro/nanogels not only to swell the particles for easy permeation of cargos,[4,5] but also for securing cargos inside either through covalent linkage[6,7] or electrostatic pairing.[8−10] However, distribution of too many charged groups from polyelectrolytes on the surface of a particle can be a drawback for intravenous applications, because the charge may cause nonspecific interaction between the particle and plasma proteins and elicit recognition by macrophages in the mononuclear phagocyte system (MPS).[11,12] Zeta-potential (ζ-potential) is generally used to characterize the surface charge of particles.[13] It is known that the higher the absolute value of ζ-potential, the more a particle tends to interact with macrophages.[14,15] Cationic particles with a high ζ-potential can also form aggregates in the presence of the negatively charged serum proteins once administered intravenously. Such aggregates can cause emboli in lung capillaries[16] and can be quickly cleared from circulation. To neutralize the surface charge while still maintaining the colloidal stability of the particle, decoration of a particle surface with poly(ethylene glycol) (PEGylation) has been extensively utilized, and proven to facilitate longer circulation times of intravenously administered particles.[11,17] Conventional PEGylation of particles either creates a dense layer of PEG that screens the surface charges[18,19] or quenches the charged groups.[20] However, neither method would work well for highly swollen hydrogel particles.

Highly swollen micro- and nanogels containing polyelectrolytes are attractive because their low modulus can enable them to navigate filtration mechanisms commonly found *in vivo*, resulting in extended blood circulation times as demonstrated in previous studies.[21−23] We used a technology

Received: January 21, 2014
Published: June 18, 2014

   dx.doi.org/10.1021/ja503939n | J. Am. Chem. Soc. 2014, 136, 9947−9952

Scheme 1. Synthetic Route from PRINT Particles to Microgels with Asymmetric Charge Distribution (Particle A to Particle D)[a]

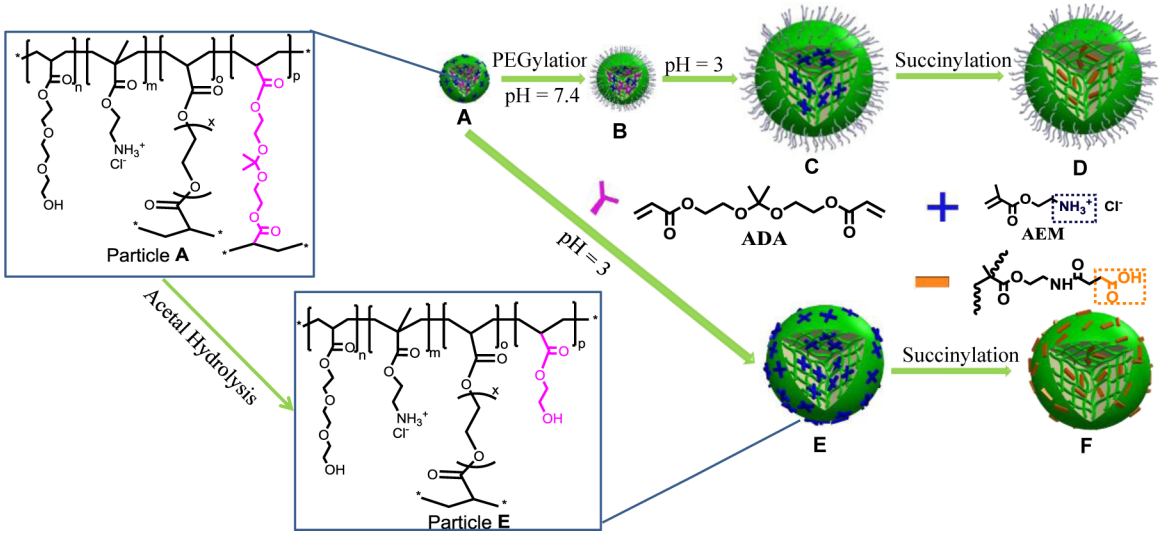

[a]Control particles with high surface charges were produced following the route of Particle **A** to Particle **F**. The schematic structures of Particle **A** and **E** are shown.

called PRINT (particle replication in nonwetting templates) to fabricate red blood cell (RBC)-like microgels (approximately 6 μm with a disk shape). PRINT is a precision micromolding technology developed in our group that can generate defined particles with controlled size, shape and chemistry, and has been extensively described in past work.[24−26] These RBC-like hydrogel particles containing carboxyl groups (Particle **I**; ζ-potential = −18 mV) had a volumetric swelling ratio Q = 30.4, with a low elastic modulus (E < 10 kPa). These particles are capable of undergoing 100% strain under physiological conditions, and demonstrated a significant (ca. 4 day) elimination half-life in mice.[21,22] They could be conjugated with significant amounts of hemoglobin (molecular weight MW = 64 kDa) to yield a potential oxygen carrier,[7] while similar particles containing amine groups as opposed to carboxyl groups may be used to scavenge nucleic acids *in vivo*.[27] A near-neutral surface charge is desired for both the carboxyl and amine containing particles toward each application.

The mesh size of a hydrogel is proportional to $Q^{1/3}$.[28] Using a modified Flory−Rehner theory presented by Peppas,[29] we calculated the mesh size in Particle **I** to be 26.6 nm (see details in Supporting Information), which also explained why hemoglobin (hydrodynamic diameter D_h = 6 nm at pH = 7.4[30]) readily diffused into the interior of Particle **I** as confirmed experimentally.[7] This large mesh size made it difficult to apply a PEG layer on the porous surface of Particle **I** to screen the surface charge. It is possible to quench the charged groups through reaction with PEG; however, these quenching molecules also had access to the interior of Particle **I**. Even for carboxyl-reactive PEG with MW of 30 kDa (D_h = 16.6 nm; see calculation in Supporting Information), we found the PEG molecules scavenged the interior carboxyl groups (Figure S8).

Herein we present a strategy to generate high-Q microgels with near-neutral surface charge while retaining charged groups (primary amines or carboxylic acids) in the interior (Scheme 1). We created highly cross-linked, minimally swollen PRINT particles containing primary amines (referred to as base Particle **A**) first, followed by selectively quenching the surface charge through PEGylation to generate surface-PEGylated base Particle **B**. Then the swelling ratio of Particle **B** was increased to produce soft hydrogel particles containing internal cationic charge (referred to as cationic-interior Particle **C**). Succinylation of primary amines in Particle **C** would convert them into carboxylic acids, resulting in particles with internal anionic charge (referred to as anionic-interior Particle **D**).

RESULTS AND DISCUSSION

The key element of our proposed synthetic strategy lies in minimizing the swelling ratio of particles during quenching of surface charge while allowing the swelling after quenching. Such a volumetric transition of particles was realized through the incorporation of transiently hydrophobic components into particles. Only after removal of these hydrophobic components post quenching would the particles swell to the desired extent.

We set out to prepare a selection of acid-labile, hydrophobic monomers for this purpose as acidic hydrolysis is a simple way to realize the hydrophobicity-to-hydrophilicity conversion.[31−33] The hydroxyl group of the hydrophilic monomer 2-hydroxyethyl acrylate (HEA) was protected using selected hydrophobic groups to generate hydrophobic monomers **1**−**3** as shown in Figure 1a. HEA has proven to be a great monomer for fabricating low modulus microgels as demonstrated in a previous study of ours.[21] These hydroxyl protecting groups

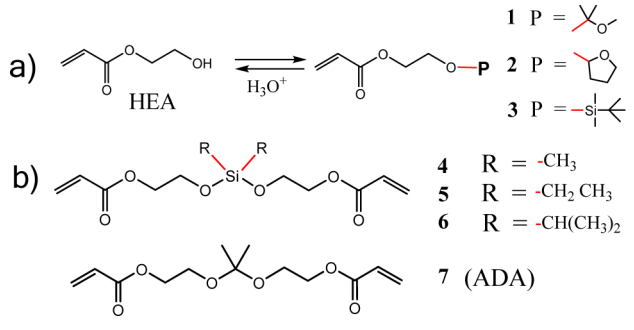

Figure 1. Structures of acid-labile, hydrophobic precursors to HEA in the form of (a) monomers (**1**−**3**) and (b) cross-linkers (**4**−**7**).

dx.doi.org/10.1021/ja503939n | J. Am. Chem. Soc. 2014, 136, 9947−9952

were chosen because the cleavage of acetal (in **1**, **2**) or silyl ether (in **3**) groups can be done in aqueous solution without requiring harsh conditions. PEG diacrylate (MW = 4000 Da; 2 wt %) was introduced as a permanent cross-linker for the hydrogel particles. The primary amine-containing monomer, 2-aminoethyl methacrylate (AEM), was copolymerized into the particles to provide a positive charge as well as a chemical handle for the PEGylation reaction. However, even with only 10 wt % AEM in the particle formulation, the resulting particles from the most hydrophobic monomer **3** still showed Q of 4.9 with an estimated mesh size of 16.2 nm.

Compared to the transient hydrophobic monomers, acid-labile cross-linkers were found to create densely cross-linked "tight" particles. Several cross-linkers derived from HEA had been considered (**4**–**7**; Figure 1b),and each of them could result in minimally swollen particles after the PRINT process. We opted for **7**, an acetal diacrylate (ADA),[34−36] because the cross-linked particles could: 1) degrade quickly at pH = 3 to swell to the desired size (<3 h, compared to >24 h for **5** and >5 d for **6**), shortening workup time; 2) stay minimally swollen without premature swelling (no obvious swelling in 3 d compared to Q = 4.1 after 6 h for **4**) in phosphate buffered saline (PBS, pH = 7.4) for storage before further reactions were carried out.

The formulation for the fabrication of ADA cross-linked Particle **A** is shown in Table S1, containing 20 wt % AEM. Using a PRINT mold with 2 μm-diameter disc-like cavities, we fabricated Particles **A** that were 2.3 ± 0.18 μm in diameter when dispersed in PBS (Figure 2a). The calculated mesh size of

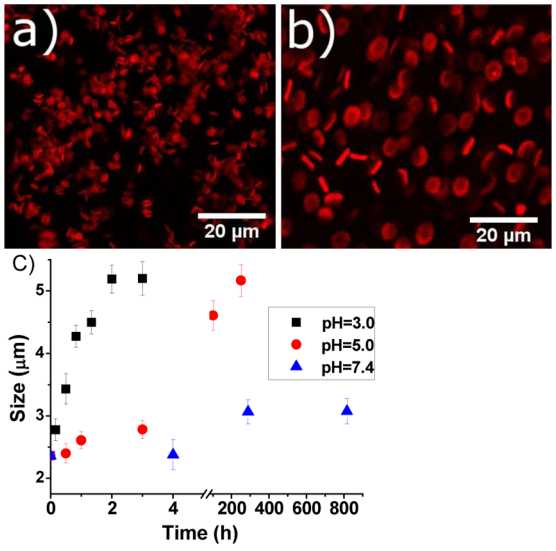

Figure 2. Fluorescent microscopic image of (a) freshly prepared Particle **A** and (b) swollen Particle **E** after acetal degradation in pH = 3 buffer for 2 h. (c) Size increase of Particle **A** overtime in different pH's. Aliquots of particle suspensions were taken out and resuspended in PBS for sizing by averaging diameter of particles under microscope (n = 50).

Particle **A** is only 1.5 nm (Q = 1.5). The size change of Particle **A** over time, due to ADA degradation at different pH's, is shown in Figure 2c. The particles could swell to a final size of ca. 5.2 μm (Figure 2b; referred to as control cationic Particle **E**) in just 2 h in pH = 3 buffer. Using FTIR (Figure S6), we confirmed that all of the acetal groups in Particle **A** could be degraded within 2 h in pH = 3 buffer.

Such a volumetric transition of hydrogel particles is possible when the dispersing medium was switched between a poor solvent for the polymer network to water. Nonpolar organic solvents can deswell hydrogel particles like Particle **I**; however, such an approach also induces severe irreversible aggregation. In our approach, the swelling of particles could be minimized without affecting the colloidal stability of particles dispersed in aqueous media.

To quench the surface charge through PEGylation without losing internal charged groups, Particle **A** was PEGylated in the "tight" state before swelling was allowed. Methoxyl PEG succinimidyl esters (mPEG-NHS) with different MWs (Table 1) were used to quench the amine groups on Particle **A**, and we

Table 1. ζ-Potential of Particles B and C When mPEG-NHS with MW of 2, 5, and 30 kDa Were Used for the PEGylation under Identical Conditions

MW of mPEG-NHS		2 kDa	5 kDa	30 kDa
ζ-potential (mV)	**B**	2.23	2.12	0.85
	C	2.54	4.86	5.27

measured the ζ-potential of the resultant Particle **B** to evaluate the efficacy of the quenching. At the same moles of mPEG-NHS used for the same weighted particles, PEG with higher MW was more efficient in screening the surface charge as the corresponding ζ-potential of Particle **B** became closer to 0 mV (Table 1). Degradation of ADA in PEGylated Particle **B** by pH = 3 buffer for 2 h led to swollen Particle **C**. However, the ζ-potential of Particle **C** showed the opposite trend against MW compared to Particle **B**. Therefore, PEGs with higher MW could shield the charge more efficiently in Particle **B**, yet were less efficient in actually quenching the amines because the larger PEG size limited grafting to the surface of Particle **B**, exposing more remaining amines on the surface in Particle **C** as demonstrated by a higher ζ-potential. To efficiently quench the surface amines while minimizing the diffusion of PEG into the interior of particles, $mPEG_{2k}$-NHS was used in the following studies.

Confocal microscopy was used to confirm that PEGylation using $mPEG_{2k}$-NHS was limited to the particle surface. This technique utilized a fluorescent probe, fluorescein-PEG_{2k}-NHS, to react with a dyeless model particle that was fabricated with the same composition as Particle **A** but in a PRINT mold with larger cavities (7 × 7 × 3 μm cylinder-shaped) for better visualization. Figure 3a displays a ring-like fluorescence pattern

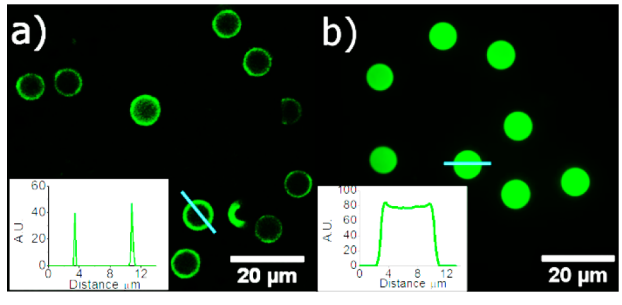

Figure 3. Confocal microscopic image of model particles (7 × 7 × 3 μm cylinders) after reaction with (a) fluorescein-PEG_{2k}-NHS and (b) fluorescein-NHS; the line scan insets show relative fluorescent intensity in particles. The molar stoichiometry of −NHS to particle was the same in both reactions.

dx.doi.org/10.1021/ja503939n | J. Am. Chem. Soc. 2014, 136, 9947−9952

present at the cross-section of these PEGylated model particles observed under a confocal microscope, indicating distribution of fluorescein-PEG$_{2k}$-NHS only on or close to the particle surface. In controls where fluorescein-NHS (MW = 473 Da) was used instead to quench the model particles under the same conditions, a disc-like fluorescence pattern was shown instead (Figure 3b). Therefore, we can infer that the quenching reaction by mPEG$_{2k}$-NHS was also limited to the surface of Particle **A**.

When carboxyl groups are preferred in the interior, the primary amines in Particle **C** could be completely converted to carboxyl groups by succinylation in 10x PBS, generating Particle **D**. The size and ζ-potential of the particles at different stages following the synthetic route from Particle **A** to **D** are summarized in Table 2. The ζ-potential was still close to neutral for Particle **D** (-5.80 ± 6.46 mV) after succinylation.

Table 2. Summary of Diameter and ζ-Potential of Particles (mPEG$_{2k}$-NHS Used for PEGylation Involved)

particle	diameter (μm)	ζ-potential (mV)
A	2.3 ± 0.18	22.8 ± 6.01
B	2.4 ± 0.22	2.23 ± 4.37
C	5.2 ± 0.33	2.54 ± 4.94
D	5.6 ± 0.29	-5.80 ± 6.46
E	5.2 ± 0.27	28.1 ± 6.49
F	5.7 ± 0.25	-32.4 ± 5.26

When Particle **A** was directly degraded without PEGylation into Particle **E**, the ζ-potential increased to 28.1 ± 6.49 mV (Table 2). Succinylation of Particle **E** reversed the charge to -32.4 ± 5.26 mV for the anionic particle referred to as control anionic Particle **F**. Using a fluorescent assay (see Supporting Information, Figure S11), we estimated that Particle **C** had 72% amine groups as that in Particle **E**. In contrast, when mPEG$_{2k}$-NHS was used to directly quench the high-Q Particle **E**, only 9.1% of the amines remained when a near-neutral surface charge was obtained. Therefore, almost 3 quarters of functional groups in the particles could be preserved using this constrained quenching method. The richness of amine and carboxyl groups in the interior of these soft microgels with a near-neutral surface charge could allow for a higher capacity for the scavenging of nucleic acids or higher conjugation of protein into the particles for our intended *in vivo* applications.

Particles with a high cationic surface are often toxic to cells.[37,38] Indeed, both Particle **A** and Particle **E** were found to be toxic when dosed to human umbilical vein endothelial cells (HUVECs), as shown in Figure 4a. When all the synthesized particles were dosed to HUVECs for 24 h with varying concentrations (from 31.25 to 1000 μg/mL), Particle **A** demonstrated toxicity starting at 62.5 μg/mL, while Particle **E** showed toxicity starting at 250 μg/mL. Particles **B** and **C**, even though containing cationic charge in the interior, did not show toxicity up to 1 mg/mL, confirming the effective quenching of surface amines. Particles **D** and **F** were not toxic as expected.

To assess the effect of the microgel surface characteristics on their interaction with macrophages, we dosed the same numbers (see Supporting Information) of different particles to the Raw 264.7 (mouse leukemic monocyte/macrophage) cell line. After incubation for 4 and 24 h, the percentage of macrophages that were associated with particles was measured by flow cytometry (Figure 4b). Particles with quenched surfaces

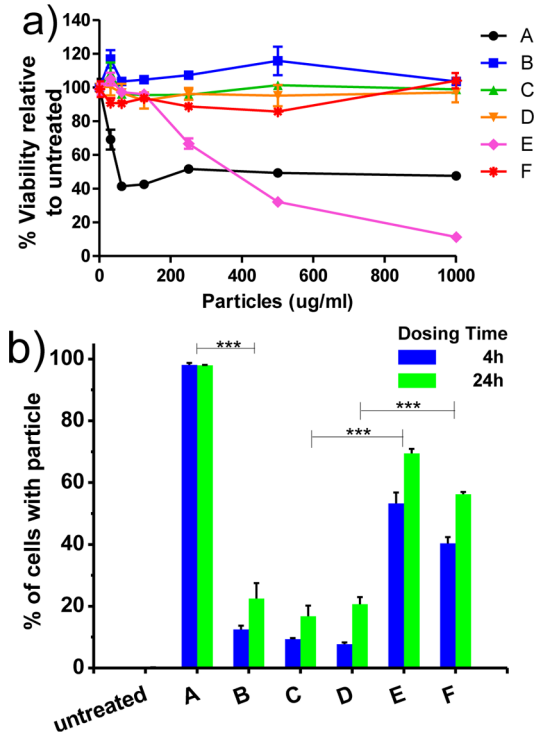

Figure 4. (a) Cytotoxicity of different particles after incubation with HUVECs for 24 h as tested by MTS assay. (n = 3 for each dose; each data point represented by mean $\pm$ SD). (b) Macrophage interaction with different particles. About 400 particles/cell dosed to a total of 10^5 Raw264.7 cells for each particle type. (Two-sided unpaired t test done among selected particles for 4 or 24 h, respectively. ***$P < 0.001$).

(Particles **B**, **C**, **D**) all showed much lower association with the macrophages than the starting cationic Particle **A** and unquenched particles (Particles **E**, **F**), indicating reduced interaction between quenched particles and macrophages.

To compare the *in vivo* performance of all of the RBC-sized soft particles, an intravital microscopic imaging method was used to observe the particles when intravenously injected into Balb/c mice. Intravital microscopy (IVM) has been used to assay the accumulation of targeted particles in tumors[39] and tissues;[40] it has also been proven to be a reliable method to evaluate the circulation times of both micro- and nanoparticles in our previous studies.[21,41,42] A near-IR (NIR) dye, DyLight 680, was copolymerized into all of the particle sets; we observed the peripheral vasculature through the skin of an anesthetized mouse's ear to track the NIR fluorescence of injected particles every 5 s for 2 h (Figure 5a). Elimination curves were generated by plotting the change in fluorescent signal from the particles over time normalizing each scan to the maximum intensity slice (Figure 5b). The mice were sacrificed after the 2 h scan and the organs were harvested for imaging to understand the distribution of the particles, expressed by percent of recovered fluorescence per gram of tissue as shown in Figure 6a.

As anticipated, particles with a quenched surface showed extended circulation times over their unquenched controls. Particle **D** demonstrated the longest circulation time of all the particles tested (Figure 5b). After 2 h, Particle **D** was highly concentrated in the spleen (Figure 6a), which is characteristic of highly deformable particles of this size (Particle **I**; Figure S14).[22] Particle **I**, which had a moderate negative surface charge (ζ-potential = -18 mV), demonstrated a very long circulation

dx.doi.org/10.1021/ja503939n | J. Am. Chem. Soc. 2014, 136, 9947−9952

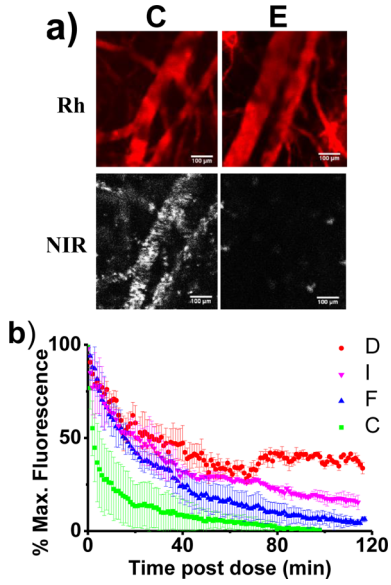

Figure 5. (a) Intravital microscopy images of mouse earlobe blood vasculature imaged at the rhodamine (Rh) channel by injecting dextran$_{70k}$-rhodamine prior to dosing particles, and imaged at the NIR channel just 100 s after dosing Particle **C** or Particle **E**. Scale bars = 100 μm. (b) Decrease in fluorescence of area of interest within 2 h of imaging by IVM (average of n = 3; mean ± SD shown every 1 min). For each particle type, 10^7 particles/g body weight were dosed.

time characterized by a distribution half-life $\alpha t_{1/2}$ of 0.6 h, and a clearance half-life $\beta t_{1/2}$ of 85.5 h calculated from conventional blood-draw method over 120 h.[22] In a 2 h scan of intravital microscopy, the circulation of Particle **I** (Figure 5b) was outperformed by Particle **D**. Therefore, it stands to infer an even longer circulation time for Particle **D** than that for Particle **I**, even though we could not calculate the half-lives from the clearance curve obtained from intravital microscopy because Particle **D** was probably still within the distribution phase during the 2 h scan.[21,41]

Negatively charged Particle **F** had a very similar biodistribution to Particle **D** (Figure 6a) and Particle **I** (Figure S14; the faster decrease in concentration than Particle **D** and **I** was probably because of clearance by the MPS system since it is known that higher charged particles attract macrophages more.[14,15] Positively charged Particle **E** was instantly removed from circulation (Figure 5a), and most of the particles ended up in the lung (Figure 6a). Since the lung is the first downstream tissue with microvasculature post injection, we could speculate that most of the dose sequestered immediately after injection of **E** because of aggregation, which is confirmed by histology of the lung (Figure 6b). Neutralizing the cationic surface charge made Particle **C** capable of circulating (Figure 5a). The bulk of the dose of Particle **C** was able to traverse the lung post injection in contrast to Particle **E** (Figure 6a,). Compared to the carboxyl-containing particles, the clearance rate of Particle **C** was fast (Figure 5b). The high porosity in Particle **C** might have allowed plasma molecules to gradually infiltrate into the particles, leading to recognition of Particle **C** by the MPS system.

CONCLUSION

To summarize, utilizing the method of PEGylation on transiently minimally swollen particles described herein, we were able to obtain highly swollen microgels with a neutral

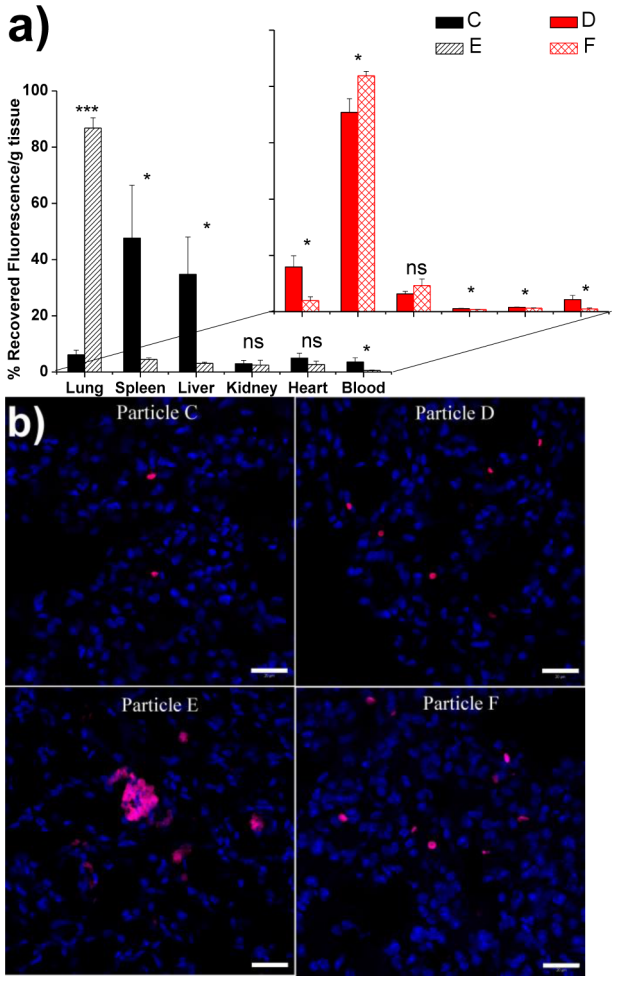

Figure 6. (a) Biodistribution of RBC-sized particles into various tissues 2 h post dosing by percent fluorescence normalized for tissue weight, with n = 3 for each case. (Two-sided unpaired t test done among selected groups. ***P < 0.001; *P < 0.05; ns, not significant.) (b) Fluorescent images of lung with nucleus stained by DAPI for mice injected with different particles (shown in purple from NIR dye). All scale bars = 20 μm.

surface charge while retaining charged groups (carboxylic acid or primary amine) in the interior. Direct PEGylation to neutralize surface charge of highly swollen microgels otherwise results in severe loss of the internal charged groups, which were desired to keep intact in order to efficiently bind cargo. These uniquely modified particles demonstrated longer circulation than their counterparts with a charged surface. The key of this strategy lies in the efficient quenching of the surface charge on "tight" particles involving a high cross-linking density using a degradable cross-linker. Even though such a volume transition was also possible through using polymers bearing a lower critical solution temperature (LCST) such as poly(*N*-isopropylacrylamide),[43] these polymers would generally stay in a collapsed state at body temperature, resulting in rigid particles. This PEGylation strategy may also be applied to other nanogel systems in which the tightness and degradation rate may be tailored by utilizing different degradable cross-linkers to achieve a balance.

dx.doi.org/10.1021/ja503939n | J. Am. Chem. Soc. 2014, 136, 9947−9952

■ ASSOCIATED CONTENT

Supporting Information

Materials, methods and instrumentation. Synthesis and characterization of molecules **1**−**7**; particle formulation; synthesis of different particles; *in vitro* and *in vivo* experiments; amine quantification method; PEG density analysis; oligonucleotide binding capacity. This material is available free of charge via the Internet at http://pubs.acs.org.

■ AUTHOR INFORMATION

Corresponding Author

desimone@unc.edu

Notes

The authors declare the following competing financial interest(s): J.M.D. is a founder and maintains a financial interest in Liquidia Technologies.

■ ACKNOWLEDGMENTS

We acknowledge the National Institutes of Health (NIH, 1R21HL092814 and 1R21HL096011), Liquidia Technologies, and Chancellor's Eminent Professorship of UNC−CH for support.

■ REFERENCES

(1) Langer, R.; Peppas, N. A. *AIChE J.* **2003**, *49*, 2990−3006.
(2) Kabanov, A. V.; Vinogradov, S. V. *Angew. Chem., Int. Ed.* **2009**, *48*, 5418−5429.
(3) Oh, J. K.; Drumright, R.; Siegwart, D. J.; Matyjaszewski, K. *Prog. Polym. Sci.* **2008**, *33*, 448−477.
(4) Kwon, H. J.; Osada, Y.; Gong, J. P. *Polymer J.* **2006**, *38*, 1211−1219.
(5) Grimshaw, P. E.; Nussbaum, J. H.; Grodzinsky, A. J.; Yarmush, M. L. *J. Chem. Phys.* **1990**, *93*, 4462.
(6) Matsumoto, N. M.; González-Toro, D. C.; Chacko, R. T.; Maynard, H. D.; Thayumanavan, S. *Polym. Chem.* **2013**, *4*, 2464.
(7) Chen, K.; Merkel, T. J.; Pandya, A.; Napier, M. E.; Luft, J. C.; Daniel, W.; Sheiko, S.; Desimone, J. M. *Biomacromolecues* **2012**, *13*, 2748−2759.
(8) Bhuchar, N.; Sunasee, R.; Ishihara, K.; Thundat, T.; Narain, R. *Bioconjugate Chem.* **2012**, *23*, 75−83.
(9) Tamura, A.; Oishi, M.; Nagasaki, Y. *J. Controlled Release* **2010**, *146*, 378−387.
(10) McAllister, K.; Sazani, P.; Adam, M.; Cho, M. J.; Rubinstein, M.; Samulski, R. J.; DeSimone, J. M. *J. Am. Chem. Soc.* **2002**, *124*, 15198−15207.
(11) Owens, D. E.; Peppas, N. a *Int. J. Pharm.* **2006**, *307*, 93−102.
(12) Verma, A.; Stellacci, F. *Small* **2010**, *6*, 12−21.
(13) Clogston, J. D.; Patri, A. K. *Methods Mol. Biol.* **2011**, *697*, 63−70.
(14) Tabata, Y.; Ikada, Y. *Biomaterials* **1988**, *9*, 356−362.
(15) He, C.; Hu, Y.; Yin, L.; Tang, C.; Yin, C. *Biomaterials* **2010**, *31*, 3657−3666.
(16) Li, S.-D.; Huang, L. *Mol. Pharmaceutics* **2008**, *5*, 496−504.
(17) Harris, J. M.; Chess, R. B. *Nat. Rev. Drug Discovery* **2003**, *2*, 214−221.
(18) Pasche, S.; Vörös, J.; Griesser, H. J.; Spencer, N. D.; Textor, M. *J. Phys. Chem. B* **2005**, *109*, 17545−17552.
(19) Hu, Y.; Xie, J.; Tong, Y. W.; Wang, C.-H. *J. Controlled Release* **2007**, *118*, 7−17.
(20) Tamura, M.; Ichinohe, S.; Tamura, A.; Ikeda, Y.; Nagasaki, Y. *Acta Biomater.* **2011**, *7*, 3354−3361.
(21) Merkel, T. J.; Jones, S. W.; Herlihy, K. P.; Kersey, F. R.; Shields, A. R.; Napier, M.; Luft, J. C.; Wu, H.; Zamboni, W. C.; Wang, A. Z.; Bear, J. E.; DeSimone, J. M. *Proc. Natl. Acad. Sci. U.S.A.* **2011**, *108*, 586−591.
(22) Merkel, T. J.; Chen, K.; Jones, S. W.; Napier, M. E.; Zamboni, W. E.; Desimone, J. M. *J. Controlled Release* **2012**, *162*, 37−44.
(23) Zhang, L.; Cao, Z.; Li, Y.; Ella-Menye, J.-R.; Bai, T.; Jiang, S. *ACS Nano* **2012**, *6*, 6681−6686.
(24) Rolland, J. P.; Maynor, B. W.; Euliss, L. E.; Exner, A. E.; Denison, G. M.; DeSimone, J. M. *J. Am. Chem. Soc.* **2005**, *127*, 10096−10100.
(25) Gratton, S. E. A.; Williams, S. S.; Napier, M. E.; Pohlhaus, P. D.; Zhou, Z.; Wiles, K. B.; Maynor, B. W.; Shen, C.; Olafsen, T.; Samulski, E. T.; Desimone, J. M. *Acc. Chem. Res.* **2008**, *41*, 1685−1695.
(26) Xu, J.; Wong, D. H. C.; Byrne, J. D.; Chen, K.; Bowerman, C.; Desimone, J. M. *Angew. Chem., Int. Ed.* **2013**, *52*, 6580−6589.
(27) Lee, J.; Sohn, J. W.; Zhang, Y.; Leong, K. W.; Pisetsky, D.; Sullenger, B. A. *Proc. Natl. Acad. Sci. U.S.A.* **2011**, *108*, 14055−14060.
(28) Canal, T.; Peppas, N. A. *J. Biomed. Mater. Res.* **1989**, *23*, 1183−1193.
(29) Peppas, N. A.; Hilt, J. Z.; Khademhosseini, A.; Langer, R. *Adv. Mater.* **2006**, *18*, 1345−1360.
(30) Papadopoulos, S.; Jürgens, K. D.; Gros, G. *Biophys. J.* **2000**, *79*, 2084−2094.
(31) Klaikherd, A.; Nagamani, C.; Thayumanavan, S. *J. Am. Chem. Soc.* **2009**, *131*, 4830−4838.
(32) Qiao, Z.-Y.; Zhang, R.; Du, F.-S.; Liang, D.-H.; Li, Z.-C. *J. Controlled Release* **2011**, *152*, 57−66.
(33) Jung, J.; Lee, I.-H.; Lee, E.; Park, J.; Jon, S. *Biomacromolecules* **2007**, *8*, 3401−3407.
(34) Cohen, J. a; Beaudette, T. T.; Cohen, J. L.; Broaders, K. E.; Bachelder, E. M.; Fréchet, J. M. J. *Adv. Mater.* **2010**, *22*, 3593−3597.
(35) Heath, W. H.; Palmieri, F.; Adams, J. R.; Long, B. K.; Chute, J.; Holcombe, T. W.; Zieren, S.; Truitt, M. J.; White, J. L.; Willson, C. G. *Macromolecules* **2008**, *41*, 719−726.
(36) Palmieri, F.; Adams, J.; Long, B.; Heath, W.; Tsiartas, P.; Willson, C. G. *ACS Nano* **2007**, *1*, 307−312.
(37) Xia, T.; Kovochich, M.; Liong, M.; Zink, J. I.; Nel, A. E. *ACS Nano* **2008**, *2*, 85−96.
(38) Goodman, C. M.; McCusker, C. D.; Yilmaz, T.; Rotello, V. M. *Bioconjugate Chem.* **2004**, *15*, 897−900.
(39) Smith, B. R.; Cheng, Z.; De, A.; Koh, A. L.; Sinclair, R.; Gambhir, S. S. *Nano Lett.* **2008**, *8*, 2599−2606.
(40) Hak, S.; Reitan, N. K.; Haraldseth, O.; Lange Davies, C. de *Angiogenesis* **2010**, *13*, 113−130.
(41) Perry, J. L.; Reuter, K. G.; Kai, M. P.; Herlihy, K. P.; Jones, S. W.; Luft, J. C.; Napier, M.; Bear, J. E.; DeSimone, J. M. *Nano Lett.* **2012**, *12*, 5304−5310.
(42) Jones, S. W.; Roberts, R. A.; Robbins, G. R.; Perry, J. L.; Kai, M. P.; Chen, K.; Bo, T.; Napier, M. E.; Ting, J. P. Y.; Desimone, J. M.; Bear, J. E. *J. Clin. Invest.* **2013**, *123*, 3061−3073.
(43) Gan, D.; Lyon, L. A. *Macromolecules* **2002**, *35*, 9634−9639.